Talanta 99 (2012) 580–585

Contents lists available at SciVerse ScienceDirect

Talanta

journal homepage: www.elsevier.com/locate/talanta

Non-covalent functionalisation of monolithic silica for the development of carbon nanotube HPLC stationary phases

Claire André, Gwenaelle Lenancker, Yves Claude Guillaume*

Univ Franche-Comté, F-25000 Besançon, France; CHU Besançon, Pôle Pharmaceutique, F-25000 Besançon, France; EA4662 Equipe Bio Analytique Synthèse (EBAS), F-25000 Besançon, France

ARTICLE INFO

Article history:
Received 27 March 2012
Received in revised form
14 June 2012
Accepted 15 June 2012
Available online 20 June 2012

Keywords:
Carbon nanotubes
Separation
HPLC
Aromatic compound

ABSTRACT

In this paper, an effective and simple method was used for the immobilization of single wall carbon nanotubes (SWCNTs) on a monolithic HPLC material containing 2 μm macropore sizes and 13 nm mesopore sizes. The chromatographic support was coated with ultra short SWCNTs in a noncovalent way to preserve the sp^2 nanotube structure and thus their physico–chemical properties. It was demonstrated that the amino-surface of the monolith stabilized with 1-methyl-2-pyrrolidinone efficiently and stably adsorbed SWCNTs onto the chromatographic support. It was shown that this novel stationary phase was very useful for the HPLC isocratic mode separation of a series of small aromatic compounds in a very short analysis time. The comparison with a classical equivalent C18 monolithic column showed that the SWCNT column presented the best efficiency in similar chromatographic conditions.

1. Introduction

The great interest of monolith or continuous bed used as separation media was that the mobile phase was forced to flow through the large pores of the medium. The silica-based monolith columns were first introduced by Nakanishi and Soga [1,2], Tanaka et al. [3] and Cabrera et al. [4]. Continuously beds made of polyacrylamide gel were introduced by Hjerten et al. [5,6]. Nevertheless, in such monolithic structures there were no small pores and thus did not permit the separation of molecules with a small size. Therefore it was necessary to develop novel monolithic structures to improve their efficiency for separation of small molecules in an isocratic mode. Due to unique properties of nanoparticles, such as their large surface-to-volume ratio and their properties that differ from those of corresponding bulk materials, the use of nanomaterials in separation science was growing rapidly [7–9]. Latex-functionalized monolithic stationary phases were developed for the separation of carbohydrates by micro-anion exchange chromatography [10] and for in-line sample preconcentration in capillary electrophoresis [11]. Silica nanoparticle-templated methacrylic acid monoliths were also used for in-line solid-phase extraction of basic analytes in capillary electrophoresis (CE) [12]. Incorporation of hydroxyapatite nanoparticles in monolithic columns were developed for separation of proteins and enrichment of phosphopeptides [13]. Gold nanoparticles were used as intermediate ligands for capillary columns with varying surface functionalities such as the preconcentration of thiol containing peptides and the separation of proteins [14–16]. Carbon nanotubes (CNTs) [17–20] were used in GC [21–27], HPLC [28–34], CE [35–38] and in capillary electrochromatography [39–41] due to the non-covalent interaction established between the analyte and these nanostructured materials including electrostatic interactions (e.g. dipole–dipole), hydrogen bonds, π–π stacking, dispersion forces, dative bonds and the hydrophobic effect. CNTs were also incorporated in porous monolithic polymer to enhance the chromatographic separation of small molecules [42] and the performance of an arginase enzymatic reactor [43]. Recently our group developed a novel HPLC column were boron nitride nanotubes (BNNTs) were entrapped into a monolithic structure for the separation of a series of aromatic compounds [44]. The interest of carbon nanotubes as mentioned in all these works was that they could improve the analytical performances of the chromatographic methods such as higher resolution and chromatographic retention or better repeatability and stability. Nevertheless, CNTs were insoluble in most common solvents and was the main obstacle of their using. As well, the use of ultra short carbon nanotubes in monolithic columns was relatively rare and remained at present time a great challenge. In this paper, to preserve the sp^2 nanotube structure and thus their physico–chemical properties ultra short SWCNTs were dynamically adsorbed on a monolithic HPLC support. The stability of this novel stationary phase was studied and

* Corresponding author. Tel.: +33 3 81 66 55 44; fax: +33 3 81 66 56 55.
E-mail address: yves.guillaume@univ-fcomte.fr (Y.C. Guillaume).

0039-9140/$ - see front matter © 2012 Elsevier B.V. All rights reserved.
http://dx.doi.org/10.1016/j.talanta.2012.06.038

its separation properties towards several small molecules were evaluated.

2. Experimental section

2.1. Equipment

The HPLC system consisted of a Waters HPLC pump 501 (Saint-Quentin, Yvelines, France), an Interchim rheodyn injection valve, Model 7125 (Interchim, Montluçon, France), fitted with a reverse 20 μL sample loop, a Merck L4000 variable-wavelength UV spectrophotometer detector, and a Merck D2500 chromato-integrator (Nogent sur Marne, France). 14 bare silica chromolith performance columns (100 mm × 4.6 mm, 2 μm macropore sizes, 13 nm mesopore sizes) were obtained from Merck KGaA (Darmstadt, Germany). Specific surface area and porosimetry of the chromatographic supports were determined by the Micromeritics ASAP 2020 Accelerated Surface Area and Porosimetry Analyzer (Micromeritics France SA, Verneuil en Halatte). The pore properties and microscopic morphology of the chromolithic supports were also analyzed using a Jeol (JSM-6380LA) analytical scanning electron microscope at 5 kV (Croissy sur Seine, France). For these last measurements, after all the chromatographic experiments, the rods were washed, cut into small pieces and then dried. A C18 silica chromolith performance column (100 mm × 4.6 mm, 2 μm macropore sizes, 13 nm mesopore sizes) was also obtained from Merck KGaA (Darmstadt, Germany).

2.2. Reagents

Water was obtained from an Elgastat water purification system (Odil, Talant, France) fitted with a reverse-osmosis cartridge. All organic solvents and test solutes were of analytical grade. Toluene, ACN, 3-aminopropyl triethoxysilane and 1-methyl-2-pyrrolidinone (NMP) were obtained from Sigma Aldrich (Saint Quentin, France). The HiPco ultra short SWCNTs (length < 10 nm (average length ~7.5 nm); residual Fe catalyst < 5% wt%) obtained by the use of a density gradient ultracentrifugation were purchased from Aldrich-Co (Paris, France). The average diameter of the nanotubes was ~1 nm. Phenol (Phe), aniline (Ani), cathecol (Cat), 4-methoxy-phenol (4MeOP), 4-ethoxy-phenol (4EtOP), 4-propioxy-phenol (4PrOP), 3-nitrophenol (3-NP), 2,3-dihydroxynaphthalene (2,3dOHNa), 1,3-dihydroxynaphthalene (1,3dOHNa), 2,3-dinitronaphthalene (2,3dNNa) and 1,3-dinitronaphthalene (1,3dNNa) were obtained from Interchim (Montluçon, France).

2.3. Methods

2.3.1. CNT immobilization process

The in situ process, which consists of the non-covalent immobilization of SWCNTs directly in pre-packed columns was used. The silanol groups of the bare silica chromolith HPLC support were silylated with 3-aminopropyl triethoxysilane. For this, the surface modification of the dried silica chromolith column was carried out with a solution of 12 μmol m^{-2} (calculated based on 300 $m^2 g^{-1}$ specific surface area of the unmodified chromolith support) of 3-aminopropyl triethoxysilane in dry toluene by pumping the reaction solution through the column at a volumetric flow rate of 0.2 mL min^{-1} for 24 h. During the reaction, the chromolith column was stored inside an HPLC oven at 70 °C. In order to remove the unreacted amount of 3-aminopropyl triethoxysilane, the column was then flushed for an additional 2 h with toluene at a volumetric flow-rate of 0.5 mL min^{-1}. The column was then washed at the same flow-rate with 60 mL of acetonitrile. It was previously demonstrated that the SWCNT coating process on amino silica surface was efficient using an 1-methyl-2-pyrrolidinone (NMP) solution [45]. Thus, by the use of this coating process, the obtained aminopropyl-silica chromolith column was then coated using a pure NMP solution (30 mL) containing x mg of SWCNTs. This coating solution was prepared by sonication using a bath-type ultrasonicator, in which the SWCNTs are almost individually dissolved at the studied concentrations. This solution was thus pumped through the column at a flow-rate of 0.1 mL min^{-1} for one night at room temperature. The consumption of SWCNTs for the column-coating was estimated by the absorbance, at 1200 nm, of the coating solution after this in situ immobilization procedure.

2.3.2. Chromatographic data determination

The retention of the aromatic compounds on the CNT-chromatographic support was evaluated using the retention factor $k=(t-t_0)/t_0$, where t was the retention time of the injected solute on the chromatogram and t_0 the column dead time determined using the mobile phase peak. The efficiency of the column reflecting the band broadening was characterized by estimating the height equivalent to a theoretical plate $h=L/(5.54(t/\delta)^2)$ where L was the column length and δ was the peak width at half-height. Moreover, the asymmetry factor A, reflecting the peak distortion, was determined by calculating the ratio of the second part of the peak over the first part of the peak at 10% of the peak height.

3. Result and discussion

3.1. SWCNT immobilization process

The in situ immobilization process was carried out on 11 bare silica chromolith columns as explained in 2.3.(1). Due to the ultra short size of the tubes (average diameter 1 nm and length- < 10 nm (average length 7.5 nm)) inferior to the size of the macropores (2 μm) and mesopores (13 nm), the tubes can penetrate these two kind of pores of the monolithic structure. For the first column x was 0 mg and corresponded to the aminopropyl-silica chromolith column (i.e., the blank column noted the $C_{0\ mg}$ column), for the second column x was 10 mg (i.e., the $C_{10\ mg}$ column) and for the last column (the eleventh) x was 90 mg (i.e., the $C_{90\ mg}$ column). Fig. 1 demonstrated that under 45 mg, the coating solution after the immobilization process contained almost no SWCNTs due to complete consumption of the SWCNTs for coating. Above 45 mg, excess SWCNTs still remained in the coating solutions and did not undergo further adsorption onto the SWCNT/aminopropyl-silica chromolithic support to form

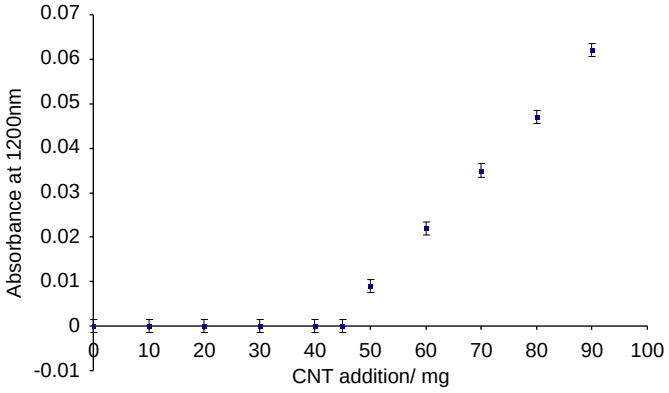

Fig. 1. Plots of absorbance at 1200 nm as a function of the SWCNT quantity x(mg) of the coating solution after the immobilization process.

Table 1
Total porosity ε_T, radius of the macropores R_P(μm), radius of the mesopores r_P(nm) and specific surface area ssa (m^2/g) values for the $C_{0\ mg}$, $C_{10\ mg}$, $C_{20\ mg}$, $C_{30\ mg}$, $C_{40\ mg}$ and the $C_{45\ mg}$ columns.

Column	ε_T	R_p (μm)	r_p (nm)	ssa (m^2/g)
$C_{0\ mg}$	0.83	2.00	13.0	300
$C_{10\ mg}$	0.81	1.96	12.8	304
$C_{20\ mg}$	0.80	1.94	12.6	310
$C_{30\ mg}$	0.79	1.92	12.3	314
$C_{40\ mg}$	0.77	1.90	12.0	318
$C_{45\ mg}$	0.76	1.88	11.9	320

multilayer SWCNTs. These results demonstrated that the minimal value of x to obtain the optimal value of covered area on the specific surface of the aminopropyl-silica chromolithic support was around 45 mg.

3.2. Characterization of the monolithic columns

The total porosity (ε_T), the specific surface area (ssa), the radius of the macropores (R_p) and mesopores (r_p) for the blank column ($C_{0\ mg}$), the optimal $C_{45\ mg}$ column and the four intermediate columns ($C_{10\ mg}$, $C_{20\ mg}$, $C_{30\ mg}$, $C_{40\ mg}$ columns) were given in Table 1. These values decreased slightly when x increased. For example, the total porosity of the prepared columns ranged from 0.76 for the optimal $C_{45\ mg}$ column which corresponded to the highest SWCNT content to 0.83 for the blank column. Higher permeabilities corresponded larger average pore diameters. As well, the relationship between the column back pressure and the x values remained linear over all the studied flow rate range with a correlation coefficient higher than 0.992. For example, $P(bars) = 0.18 \times (mg) + 82.92$ ($r^2 = 0.999$) at 5 mL/min. This column back pressure increased slightly when x increased confirming the fact that the size of both macro and mesopores decreased slightly due to the ultrathin layer of SWCNT for the coating of the aminopropyl-silica chromolithic structure. Later in this paper the studied column was now the optimal column i.e., the $C_{45\ mg}$ column.

3.3. Stability of the $C_{45\ mg}$ column

To evaluate the column to column reproducibility, three $C_{45\ mg}$ columns were prepared under identical conditions as described above. The retention factors (with standard deviations in parentheses) were obtained with Phe 0.21(0.02), 4EtOP 2.00(0.01) and 1,3dNNa 6.22(0.04) used as tested analytes. The mobile phase was an ACN/H_2O (55/45) (v/v) mixture with a flow rate of 1 mL/min and a column temperature equal to 25 °C. The results showed that the technique was reliable and reproducible. As well, typical reproducibility of this column in retention time measured as relative standard deviation was $< 0.4\%$. After half a year and more than 50 times injections, the decrease for the values of retention factor on this column was $< 1.2\%$. Three endurance tests concerning the $C_{45\ mg}$ column stability over firstly a wide temperature range (Fig. 2), secondly over a wide ACN fraction range in the ACN/water mixture (Fig. 3) and thirdly over a wide mobile phase flow-rate (Fig. 4) were also carried out. The test solute used was 4EtOP. As can be seen, although changes in retention are expected with temperature and ACN fraction in the mobile phase (Figs. 2 and 3), the stability of the column over a wide temperature and ACN fraction is evident. As well, the column stability is excellent over a wide flow-rate (Fig. 4). As well, Fig. 5 represented the variation of the $C_{45\ mg}$ column back pressure versus the flow-rate. An excellent linear dependence was observed which clearly demonstrated that the $C_{45\ mg}$ column was mechanically stable.

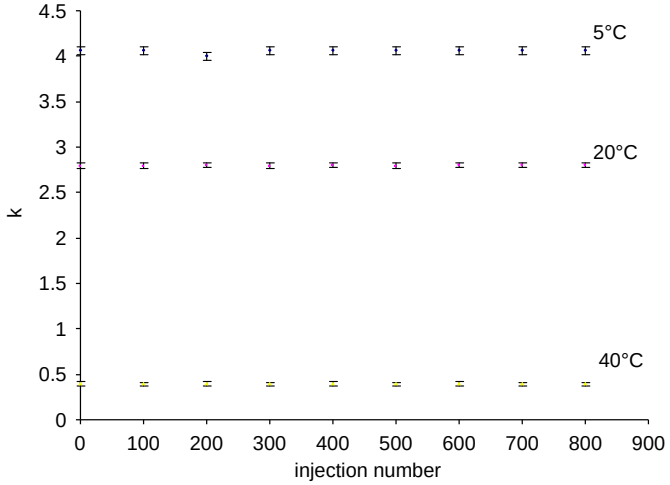

Fig. 2. k versus the injection number of 4EtOP at 5 °C, 20 °C and 40 °C. Column: $C_{45\ mg}$. Mobile phase: ACN/H_2O (55/45)(v/v). Flow rate: 1 mL/min. Detection wavelength: 254 nm.

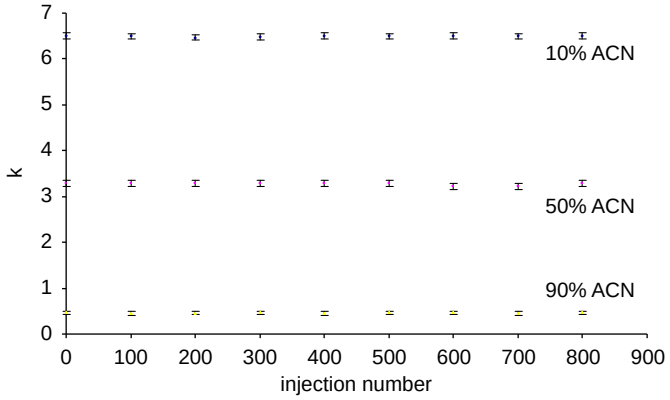

Fig. 3. k versus the injection number of 4EtOP at 10%, 50% and 90% of ACN in a ACN/Water mixture as mobile phase. Column: $C_{45\ mg}$. Flow rate: 1 mL/min. Column temperature: 25 °C. Detection wavelength: 254 nm.

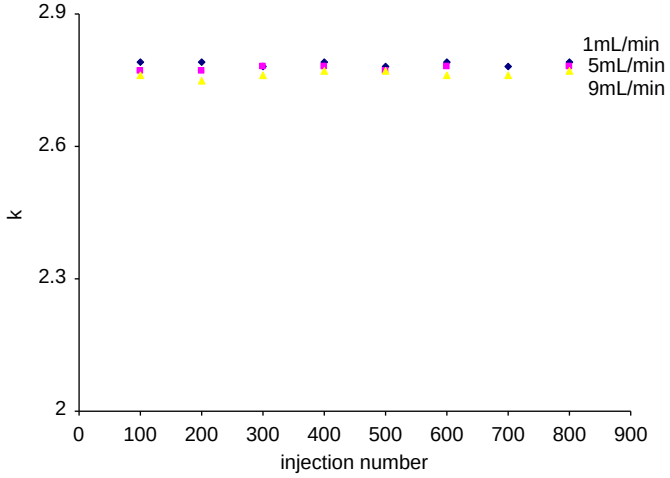

Fig. 4. k versus the injection number of 4EtOP at 1 mL/min, 5 mL/min and 9 mL/min. Column: $C_{45\ mg}$. Mobile phase: ACN/H_2O (55/45)(v/v). Column temperature: 25 °C. Detection wavelength: 254 nm.

The effect of long-term storage (for six months) under the mobile phase conditions were also determined. A long-term storage did not significantly affect the retention properties of the $C_{45\ mg}$ column.

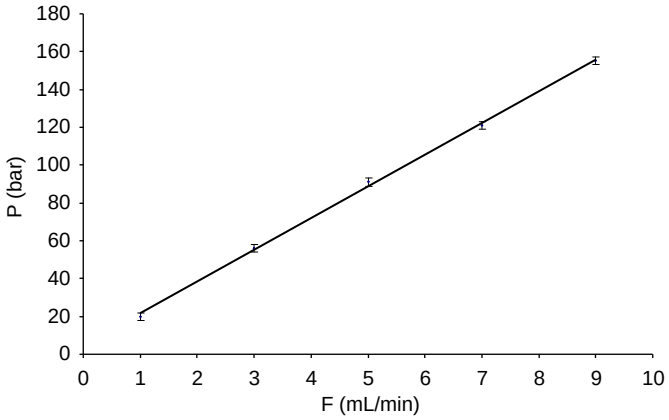

Fig. 5. *P*(bar) versus *F*(mL/min) for the $C_{45\ mg}$ column. Mobile phase: ACN/H_2O (55/45)(v/v). Column temperature: 25 °C.

Table 2
Retention factor *k*, peak asymmetry *A*, plate height *h* (μm) and Δ*H* (kJ mol^{-1}) values for the binding mechanism of the solute molecules with the SWCNT stationary phase ($C_{45\ mg}$ column).

Solute · molecule	*k*	*A*	*h* (μm)	Δ*H* · (kJ mol^{-1})
Phe ·	0.21	1.00	3.87	−10.4
Ani	0.60	1.00	3.76	−12.7
Cat	0.81	1.00	3.89	−15.4
4MeOP	1.31	1.00	3.78	−20.2
4EtOP	2.00	1.00	3.96	−24.5
4PrOP	2.72	1.00	4.00	−29.8
3NP	3.07	1.00	3.98	−40.7
2,3dOHNa	5.29	1.00	3.99	−60.8
1,3dOHNa	5.49	1.00	4.01	−61.7
2,3dNNa	5.76	1.00	3.88	−63.5
1,3dNNa	6.22	1.00	3.97	−70.5

Mobile phase: ACN/H_2O (55/45)(v/v). Flow rate: 1 mL/min. Column temperature: 25 °C. Detection wavelength: 254 nm.

3.4. Solute molecule association mechanism with the $C_{45\ mg}$ column

The retention factor (*k*) the asymmetry factor (*A*) and the column plate height (*h*) of the chromatographic peak of the $C_{45\ mg}$ column were evaluated using the eleven aromatic compounds as probe solutes (Table 2). With the $C_{45\ mg}$ column, the retention factor obtained was in the sequence: Phe < Ani < Cat < 4MeOP < 4EtOP < 4PrOP < 3NP < 2,3dOHNa < 1,3dOHNa < 2,3dNNa < 1,3dNNa. Phenol was eluted first, followed by aniline and cathecol which contained a second –OH group in its ring. Similar retention behavior was observed on the porous graphitic carbon PGC surface [46]. This polar retention effect on SWCNT was due to different intermolecular interactions, including electron pair donor-electron pair acceptor (charged transfer) and dipole–dipole interactions. Among the phenol derivatives, 3NP presented the strongest retention. Indeed, the substitution of the –OH group for catechol with a $-NO_2$ substituent had the strongest van der Waals and polar interactions with the CNT surface. As well, it appeared that this SWCNT chromolith column had the highest affinity for the naphthalene derivatives. This result confirmed that a planar conformation was important for the retention on the SWCNT stationary phase [29,30]. The aromatic rings of the naphthalene derivatives exhibited with the CNT surface favorable interactions. To gain further insight into this molecule—CNT chromolith association mechanism the previous experiments were carried out at four other temperatures (i.e., 5 °C, 10 °C, 30 °C, 40 °C). The molecule-SWCNT chromolith association mechanism enthalpy (ΔH°) was calculated using the slopes (*P*) of the linear plots lnk vs (1/*T*) (van'T Hoff plots; $r^2 > 0.9988$) i.e., $\Delta H^\circ = -R.P$ where $R = 8.32$ J/mol/K. Table 2 presents the ΔH° values for all molecules. The interaction enthalpies for all the solute molecules with CNT were exothermic and consequently favorable for their association with CNT. As well, it was observed that the enthalpy value determined on the CNT phase was the lowest for naphtalene derivatives. This confirmed that the SWCNT immobilized on the chromolithic surface exhibited with aromatic rings favorable non-specific interactions and increased the retention of compounds containing aromatic rings in their molecular structure. This result was also supported by an inversion of the retention order, in similar chromatographic conditions, of the solute molecules on the C18 commercial chromolith stationary phase, i.e 3NP < Cat < Ani < Phe < 1,3dNNa < 2,3dNNa < 1,3dOHNa < 2,3dOHNa < 4MeOP < 4EtOP < 4PrOP. This increase in the polar interactions is related to the CNT structure which can be viewed as graphite sheet (sp^2) carbon that has been rolled up into a tiny tube. There is thus growing evidence to suggest that polar interactions have a significant influence on retention. The mechanism of this effect must be elucidated, but it is possibly due to π–π stacking interactions between aromatic solutes and the single walled carbon nanotubes of the CNT phase. As well, since the nanotubes are full of π electrons the aromatic ring of a solute molecule is likely to interact with the surface of tubes through ═CH–π hydrogen bonds as previously demonstrated for polycyclic aromatic hydrocarbons [32]. As well, the retention order of the alkyl oxy phenol (i.e., an increase in retention was observed with the number of carbon atom on the alkyl chain) on the SWCNT chromolith column can be explained by the fact that hydrophobic effects additive to the polar interactions were implied in the molecule association mechanism on SWCNT. This result was confirmed by the fact that increasing the ACN percentage in the mobile phase reduces the retention factor on the SWCNT stationary phase for the whole solute molecules in the mixture (Fig. 3).

3.5. SWCNT/monolithic column efficiency

The separation of the solute molecules on the two columns i.e., the commercial C18 monolithic column (C18C) and the SWCNT monolithic column ($C_{45\ mg}$) was now analyzed. The resolution *Rs* for the worst separated pair of peaks on the chromatogram and the analysis time ta were plotted versus the ACN fraction in the mobile phase for a temperature equal to 25 °C at high flow-rate 8.5 mL/min. Fig. 6 showed an optimal separation (*Rs* = 1.5) for an acetonitrile fraction equal to 60% with a low analysis time. The corresponding chromatogram was given in Fig. 7. Due to mass transfert properties of the monolithic skeleton the 11 compounds can be baseline separated within 2 min with a total system back

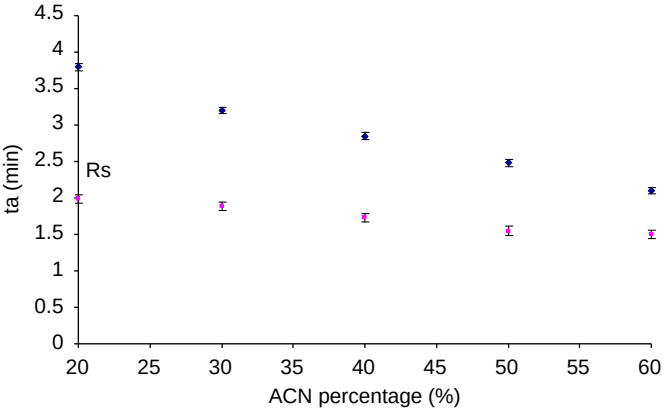

Fig. 6. Separation analysis time (min) and resolution *Rs* for the worst separated pair of peaks on the chromatogram versus the ACN fraction in the ACN/H_2O mobile phase. Column: $C_{45\ mg}$. Flow rate: 8.5 mL/min. Column temperature: 25 °C. Detection wavelength: 254 nm.

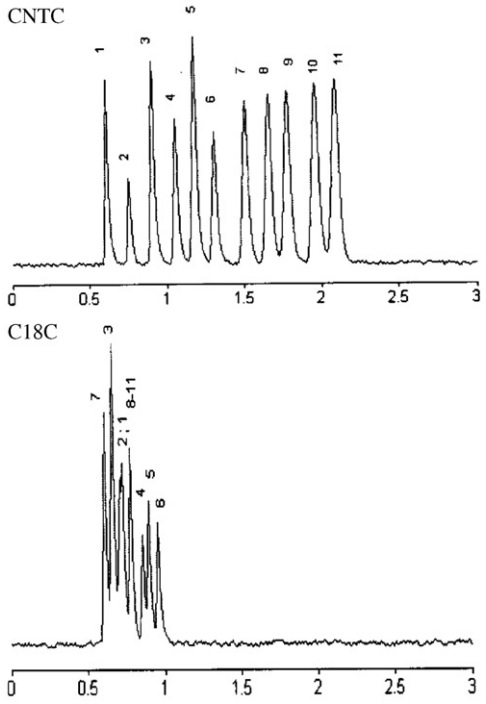

Fig. 7. HPLC chromatograms for the separation of *(1) Phe; (2) Ani; (3) Cat; (4) 4MeOP; (5) 4EtOP; (6) 4PrOP; (7) 3NP; (8) 2,3dOHNa; (9) 1,3dOHNa; (10) 2,3dNNa; (11) 1,3dNNa on the $C_{45\ mg}$ column and the commercial C18 column (C18C). Chromatographic conditions: Mobile phase: ACN/H_2O (60/40)(v/v). Flow rate: 8.5 mL/min. Column temperature: 25 °C. Detection wavelength: 254 nm (*number refers to peak on the chromatograms).

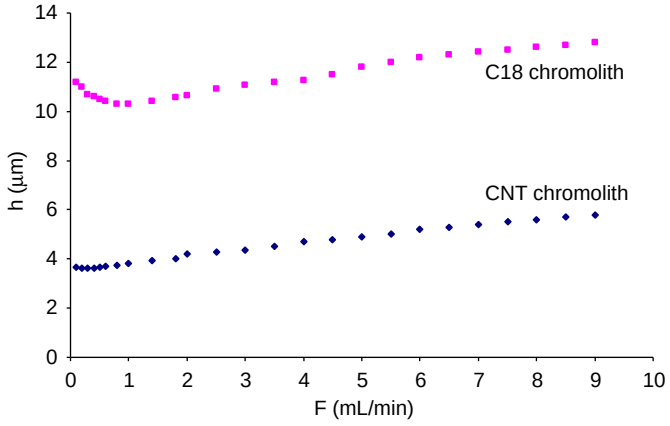

Fig. 8. Plot of the height equivalent to a theoretical plate h(µm) vs flow-rate F(mL/min) for the $C_{45\ mg}$ column (SWCNT chromolith) and the equivalent classical C18 chromolith performance column (C18C); injected solute: 4EtOP. Mobile phase: ACN/H_2O (55/45)(v/v). Column temperature: 25 °C. Detection wavelength: 254 nm.

pressure of 150 bars. In similar chromatographic conditions the 11 compounds were not separated on the C18 commercial chromolith column (Fig. 7). Sharp and symmetrical peaks were obtained for all peaks. Fig. 8 showed the variation of the height equivalent to a theoretical plate (h(µm)) versus the flow-rate F(mL/min) for the SWCNT monolithic column and for the commercial chromolith C18 column furnished by Interchim. To show more clearly the minimum plate height on the SWCNT column, the variation of the height equivalent to a theoretical plate (h(µm)) versus the flow-rate F(mL/min) was given in Fig. 9 for a flow-rate variation between 0.1 mL/min and 1 mL/min. Fig. 8 showed that the lowest efficiency was observed for the C18 chromolith column. The minimum plate height

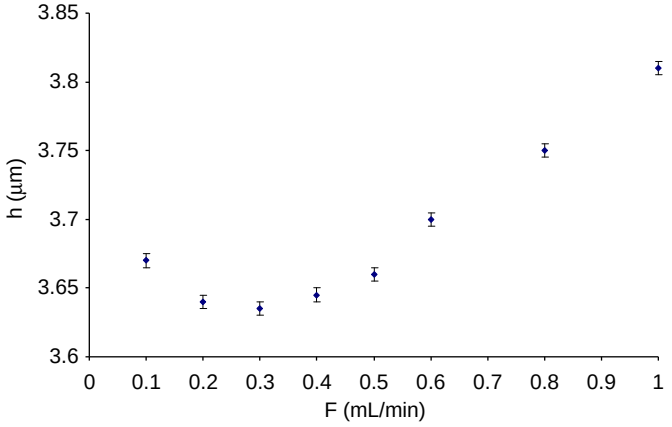

Fig. 9. Plot of the height equivalent to a theoretical plate h(µm) vs flow-rate F(mL/min) in the 0.1 mL/min-1 mL/min range for the $C_{45\ mg}$ column (SWCNT chromolith) and the injected solute: 4EtOP. Mobile phase: ACN/H_2O (55/45)(v/v). Column temperature: 25 °C. Detection wavelength: 254 nm.

was for the C18 column around 10 µm at 1 mL/min as usually described in the literature [47–49]. For the SWCNT monolithic column the minimum plate height was around 3.6 µm at 0.3 mL/min (Fig. 9). As well, Fig. 8 demonstrated clearly that the separation efficiency did not decrease significantly when the flow rate was increased as was the case with traditional particulate columns. This result confirmed that using this novel SWCNT column, it was possible to operate at high flow rates with no loss of peak resolution as it was observed on Fig. 7.

4. Conclusion

This paper described a controlled and specific in-situ method for immobilizing ultra short carbon nanotubes with unperturbed sp2 structures and electronic properties on a chromolith chromatographic support. This simple immobilization method enabled the development of a stable stationary phase which exhibited efficient separation at high flow-rate values with no loss of peak resolution.

References

[1] K. Nakanishi, N. Soga, J. Am. Ceram. Soc. 74 (1991) 2518–2530.
[2] K. Nakanishi, N. Soga, J. Non-Cryst. Solids 139 (1992) 1–13.
[3] H. Minakuchi, K. Nakanishi, N. Soga, N. Ishizuka, N. Tanaka, Anal. Chem. 68 (1996) 3498–3501.
[4] K. Cabrera, G. Wieland, D. Lubda, K. Nakanishi, N. Soga, H. Minakuchi, K.K. Unger, Trends Anal. Chem. 17 (1998) 50–53.
[5] S. Hjerten, J.L. Liao, R. Zhang, J. Chromatogr. 473 (1989) 273–275.
[6] J.L. Liao, R. Zhang, S. Hjerten, J. Chromatogr. 586 (1991) 21–26.
[7] C. Nilsson, S. Nilsson, Electrophoresis 27 (2006) 76–83.
[8] C. Nilsson, S. Birnbaum, S. Nilsson, J. Chromatogr. A 1168 (2007) 212–224.
[9] Z. Zhang, Z. Wang, Y. Liao, H. Liu, J. Sep. Sci. 29 (2006) 1872–1878.
[10] E.F. Hilder, F. Svec, J.M.J. Frechet, J. Chromatogr. A 1053 (2004) 101–106.
[11] J.P. Hutchinson, P. Zakaria, A.R. Bowiet, Anal. Chem. 77 (2005) 407–416.
[12] J.R.E Thabano, M.C. Breadmore, J.P. Hutchinson, J. Chromatogr. A 1216 (2009) 4933–4940.
[13] J. Krenkova, A. Lacher Nathan, F. Svec, Anal. Chem. 82 (2010) 8335–8341.
[14] Y. Xu, Q. Cao, F. Svec, J.M.J. Frechet, Anal. Chem. 82 (2010) 3352–3358.
[15] Q. Cao, Y. Xu, F. Liu, F. Svec, J.M.J. Frechet, Anal. Chem. 82 (2010) 7416–7421.
[16] D. Connoly, B. Twamley, B. Paull, Chem. Commun. 46 (2010) 2109–2111.
[17] S.Q. lijima, Nature 354 (1991) 56–58.
[18] H. Uchiyama, K. Kaneko, S. Oseki, J. Chem. Soc. 85 (1987) 4326–4333.
[19] S.Q. Lijima, T. Ichibashi, Nature 363 (1993) 603–605.
[20] D.S. Bethune, C.H. Klang, M.S. De Vries, G. Gorma, R. Savoy, J. Vasquez, R. Beyers, Nature 363 (1993) 605–607.
[21] Q.L. Li, D.X. Yuan, J. Chromatogr. A 1003 (2003) 203–209.
[22] C. Saridara, S. Mitra, Anal. Chem. 77 (2005) 7094–7097.
[23] M. Karwa, S. Mitra, Anal. Chem. 78 (2006) 2064–2070.

[24] M. Stadermann, A.D. McBrady, B. Dick, V.R. Reid, A. Noy, R.E. Synovec, O. Bakajin, Anal. Chem. 78 (2006) 5639–5644.
[25] L.M. Yuan, R.N. Ren, L. Li, P. Ai, Z.H. Yan, Z. Zi, Y. Li, Anal. Chem. 78 (2006) 6384–6390.
[26] L. Zhao, P. Ai, A.H. Duan, L.M Yuan, Anal. Bioanal. Chem. 399 (2011) 143–147.
[27] A. Speltini, D. Merli, E. Quartarone, A. Profulo, J. Chromatogr. A 1217 (2010) 2918–2924.
[28] Y. Li, Y. Chen, R. Xiang, D. Ciuparu, L.D. Pfefferle, C. Horvath, J.A. Wilkins, Anal. Chem. 77 (2005) 1398–1406.
[29] C. Andre, T. Gharbi, Y.C. Guillaume, J. Sep. Sci. 32 (2009) 1757–1764.
[30] C. Andre, R. Aljhni, T. Gharbi, Y.C. Guillaume, J. Sep. Sci. 34 (2011) 1221–1227.
[31] E. Menna, F. Della Negra, M. Prato, N. Tagmatarchis, A. Ciogli, F. Gasparrrini, D. Misita, C. Villani, Carbon 44 (2006) 1609–1613.
[32] Y.X. Chang, L.L. Zhou, G.X. Li, L. Li, L.M. Yuan, J. Liq. Chromatogr. Related Technol. 30 (2007) 2953–2958.
[33] S.H. Kwon, J.H. Park, J. Sep. Sci. 29 (2006) 945–952.
[34] Y.X. Chang, C.X. Ren, Q. Ruan, L.M. Yuan, Chem. Res. Chin. Univ. 23 (2007) 646–649.
[35] Y. Xu, S.F.Y. Li, Electrophoresis 27 (2006) 4025–4048.
[36] Y. Moliner-Martinez, S. Cardenas, M. Valcarcel, Electrophoresis 28 (2007) 2573–2579.
[37] J.M. Jimenez-Soto, Y. Moliner-Martinez, S. Cardenas, M. Valcarcel, Electrophoresis 31 (2010) 1681–1688.
[38] B. Suarez, B.M. Simonet, S. Cardenas, M. Valcarcel, Electrophoresis 28 (2007) 1714–1722.
[39] L. Sombra, Y. Moliner-Martinez, S. Cardenas, M. Valcarcel, Electrophoresis 29 (2008) 3850–3857.
[40] J.H.T. Luong, P. Bouvrette, Y. Liu, D.Q. Yang, E. Sacher, J. Chromatogr. A 1074 (2005) 187–194.
[41] J.L. Chen, J. Chromatogr. A 1217 (2010) 715–721.
[42] S.D. Chambers, F. Svec, J.M.J. Frechet, J. Chromatogr. A 1218 (2011) 2546–2552.
[43] C. Andre, D. Agiovlasileti, Y.C. Guillaume, Talanta 85 (2011) 2703–2706.
[44] C. Andre, Y.C. Guillaume, Talanta, in press.
[45] T. Fujigaya, J.T. Yoo, N. Nakashima, Carbon 49 (2011) 468–476.
[46] Y.C. Guillaume, T.T. Truong, J. Millet, L. Nicod, J.C. Rouland, M. Thomassin, J. Chromatogr. A 955 (2002) 197–205.
[47] A.M. Siouffi, J. Chromatogr. A 1126 (2006) 86–94.
[48] K. Cabrear, G. Wieland, D. Lubda, K. Nakanishi, N. Soga, H. Minaguchi, et al., Trends Anal. Chem. 17 (1998) 50–53.
[49] M. Kele, G. Guiochon, J. Chromatogr. A 960 (2002) 19–49.